Lithium Silicates Nanosheets with Excellent Capture Capacity and Kinetics with Unprecedented Stability for High-Temperature CO_2 Capture

Rajesh Belgamwar,[a] Ayan Maity,[a] Tisita Das,[b] Sudip Chakraborty,[b] Chathakudath P. Vinod,[c] Vivek Polshettiwar[a]*

[a]Department of Chemical Sciences, Tata Institute of Fundamental Research (TIFR), Mumbai, India. Email: vivekpol@tifr.res.in
[b]Discipline of Physics, Indian Institute of Technology (IIT) Indore, India
[c]Catalysis and Inorganic Chemistry Division, CSIR-National Chemical Laboratory (NCL), Pune, India

EXPERIMENTAL

Characterization. SEM imaging was performed on a ZEISS ULTRA field emission scanning electron microscope. The SEM was operated with an accelerating voltage at 3 to 5kV. SEM samples were prepared by the drop-casting diluted ethanolic suspension of the powder onto the aluminum stub. The Brunauer-Emmet-Teller (BET) Nitrogen adsorption studies were performed on Micromeritics 3-Flex analyzer. The sample tubes were filled with approximately 100 mg of samples and then degassed for 12 h at 120 °C using an external degasser. Then the tubes were attached to the analyzer, and before starting the analysis, it was again degassed at 120 °C for 2 h to removal all moisture and adsorbed gases. X-ray diffraction patterns were recorded using Panalytical X'Pert Propowder X-ray diffractometer using Cu-Kα radiation.

The XPS and depth profile analysis was carried out using Thermoscientific Kalpha+ spectrometer fitted with monochromatic Aluminum Kα x-ray source (1486.6 eV). The charge neutralization gun was always switched on during the data collection. The spot size of the x-ray was 400 microns. Depth profile analysis was carried out with Argon sputter source at 1000 eV ion energy. In total, 16 layers of etching were carried out, with each layer constituting 60 seconds followed by data acquisition. So a total of 960 seconds of etching experiment was carried out on each sample with an etch rate of 0.282 nm per second, making a profile of approximately 270 nm. The data was analyzed using Avantage software with peak fitting done with a Gaussian- Lorentzian peak type using Shirley background.

Synthesis of Lithium Silicate Nanomaterial. In a 500 mL beaker, lithium precursor (15.4 g) was dissolved in 255 mL of water and hydrolyzed by slowly adding aqueous ammonia solution by bringing the solution pH to 8[1]. DFNS (3.3 g) was then dispersed in 50 mL water by sonication for 30 min and then was slowly added to lithium precursors solution (Li:Si ratio was 4.66:1), at room temperature and stirred for 1 h,. This solution was then left for 24 h without stirring. It was then heated at 120 °C under stirring until all the solvent was evaporated to obtain dry white powder. Then 1.6 g of this powder and grinded using mortar and pestle and heated in a furnace at 650 °C with 10 °C /min ramp and maintained at 650 °C for 6 h. The white powder was obtained, named as as-prepared LSN.

CO_2 Capture Studies. The CO_2 capture by LSN was carried out by using thermogravimetric analysis (TGA) Mettler Toledo TGA-DSC2/LF/1100. 25 mg of LSN was taken in TGA crucible with 1cm diameter and 400 µL volume. The gases were feed by the mass flow controller. First, LSN was heated to 650 °C with 10 °C/min ramp under the nitrogen flow of 50 mL min^{-1}. Once the temperature reached to 650 °C, after 10 min of stabilization, the flow of gas was changed from nitrogen to CO_2: N_2 (60:40) gas mixture with a flow of 150 mL min^{-1}. Weight gain due to CO_2 adsorption was monitored with time for 2 h at 650 °C. The adsorption capacity of the sorbent in weight (wt)% was calculated based on the total weight gain during the CO_2 sorption step and kinetics based initial CO_2 capture capacities of LSN in the first minute. For CO_2 desorption, the sorbent was heated to 650 °C under the nitrogen flow of 150 mL min^{-1} for 20 min. For the cyclic stability study, adsorption-desorption cycles were repeated up to 200 times under exactly the same conditions Scheme 1. For different CO_2 concentrations, we only changed the ratio of CO_2: N_2 and for different sorbents weight, we only changed the weight of the sorbent and other conditions were kept the same.

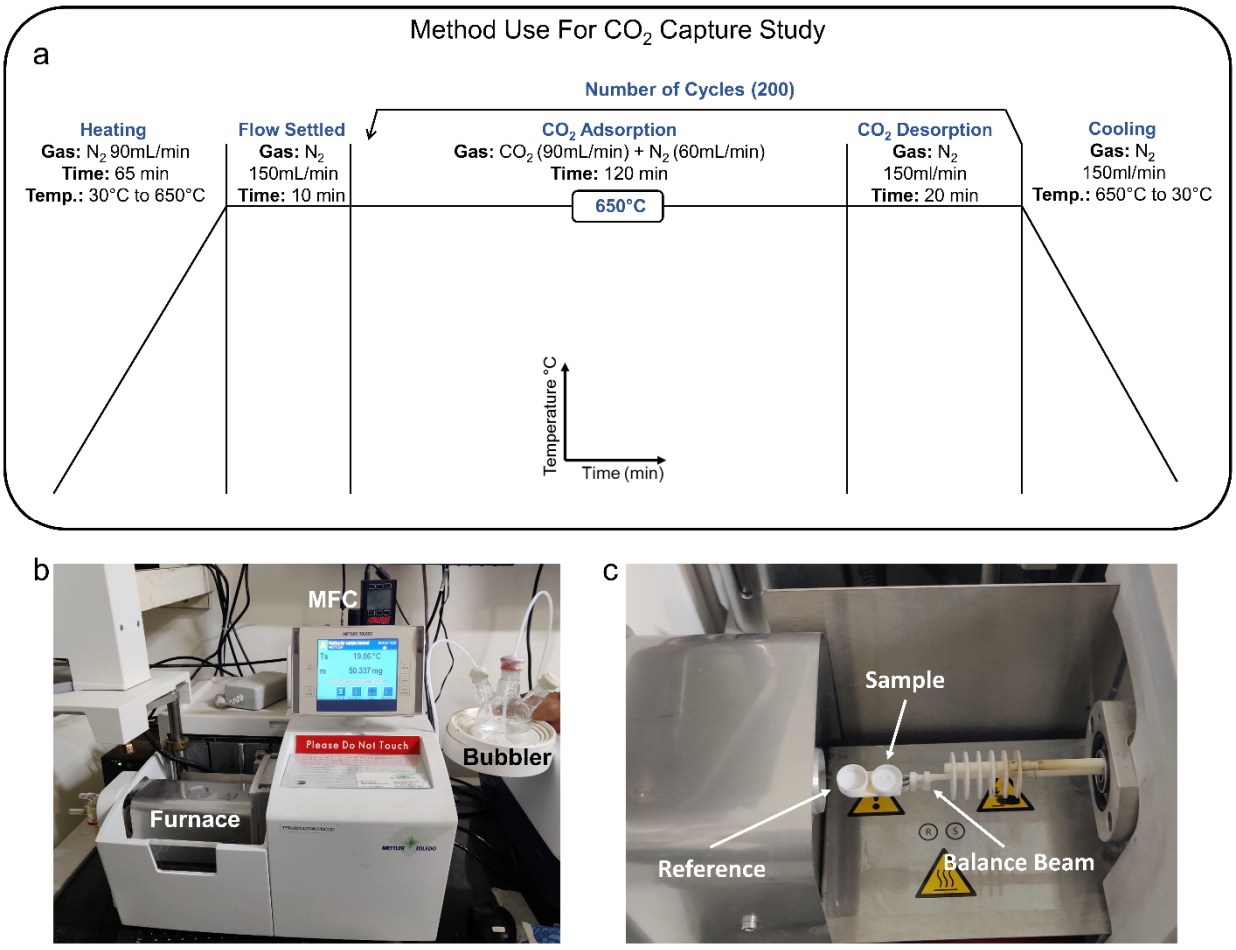

Instrument Details: TGA-DSC2/LF/1100
Maximum Operating Temperature 1200 °C

Scheme S1. a) Schematic of method used for high-temperature CO_2 capture, b) Image of TGA instrument with bubbler and c) Furnace and sample holder details.

Computational Details. All the DFT calculations for geometry optimization and electronic structure prediction are carried out using Vienna *ab-initio* Simulation Package (VASP) code in conjunction with projector augmented wave (PAW) formalism. Plane wave basis set with a kinetic energy cut-off of 500 eV has been used. The exchange-correlation part is approximated by using Perdew, Burke and Ernzerhof (PBE) type generalized gradient approximation (GGA). The standard Monkhrost-Pack grid with 5×5×1 k-mesh has been used to sample the brillouin zone. For all the total energy calculations performed in this work, self-consistency is achieved with a convergence criterion of 1 meV (10^{-3} eV), while the force tolerance criterion for Hellman–Feynman forces among the constituent atoms is set to $1x10^{-2}$ eV/Å. The van der Waals effect has been incorporated by using Grimme's method of DFT-D3 dispersion correction for all the surface calculations. In order to avoid the interaction between two adjacent images, a vacuum of ~15 Å has been used along the Z direction.

Our first-principles based study enables to visualize and explain the adsorption-desorption mechanism from the electronic structure perspective and thus is expected to provide strong validation of the experimental findings. In order to further explain the nature of the adsorption, we have analyzed the electron density distribution between the surface and adsorbate through the Bader charge analysis as per the following equation:

$$\Delta\rho = \rho[\text{LSN-CO}_2] - \rho[\text{LSN}] - \rho[\text{CO}_2] \quad (1)$$

where, $\rho[\text{LSN-CO}_2]$, $\rho[\text{LSN}]$ and $\rho[\text{CO}_2]$ are the charge density of CO_2 adsorbed LSN composite, free LSN substrate and isolated CO_2 molecule, respectively. In addition to the qualitative analysis of the electron density distribution, we have also validated our observation from the quantitative confirmation of the charge transfer mechanism based on the Bader charge analysis. For a deeper theoretical analysis and a more detailed picture of CO_2 adsorption/desorption characteristics, we have also determined the work function of all the considered surfaces, including Li_4SiO_4 with and without adsorbed CO_2, Li_2SiO_3 and Li_2CO_3, which are summarized in figure 7c. To begin with, we have investigated the interaction between free-standing Li_4SiO_4 nanosheet and CO_2 molecule. For that, the model structure is simulated through Li_4SiO_4 bulk optimization and subsequent construction of the lithium silicate nanosheet (LSN), while adding a vacuum of 15 Angstrom along 001 direction. We have considered Li_4SiO_4 unit cell containing 56 Li, 14 Si and 56 O atoms. For the adsorption study, we have kept CO_2 molecule initially on top of LSN at ~ 2.3 Å distance, which after full ionic relaxation reduced to ~2.14 Å through a Li-O bond formation.

Table S1. CO_2 capture performance of LSN synthesized using various Li-precursors at 650 °C in air for 6h

Li: Silica Precursor	**Mole Ratio of Li: Si Precursor**	**CO_2 Capture in 1st cycle (Wt. %) at 650 °C**
$LiNO_3$: DFNS	4.66: 1	28.5 %
Li_2CO_3: DFNS	6.6: 1	10 %
LiOH: DFNS	6.6: 1	6.3 %

Table S2. CO_2 capture performance of LSN synthesized using DFNS and $LiNO_3$ with different mole ratios at 650 °C in air for 6h

Precursors used	Mole Ratio of Li: Si Precursor	CO_2 Capture in 1st cycle (Wt. %) at 650 °C
$LiNO_3$: DFNS	4.66: 1	28.5 %
$LiNO_3$: DFNS	6.66: 1	19.8 %
$LiNO_3$: DFNS	11.6: 1	24.23 %

Table S3. CO_2 capture performance of LSN synthesized using DFNS and $LiNO_3$ with different mole ratios at 650 °C in air, with different thermal treatment time.

Precursors used	Molar Ratio Precursors	Thermal Treatment (at 650 °C in the air) Time	CO_2 Capture in 1st cycle (Wt. %) at 650 °C
$LiNO_3$: DFNS	4.66: 1	6h	28.5 %
$LiNO_3$: DFNS	7.66: 1	6h	19.8 %
$LiNO_3$: DFNS	11.6: 1	6h	24.23 %
$LiNO_3$: DFNS	16.6: 1	6h	21.9 %
$LiNO_3$: DFNS	4.66: 1	12h	16.6 %
$LiNO_3$: DFNS	7.66: 1	12h	19.87 %
$LiNO_3$: DFNS	16.6: 1	12h	22 %

Table S4. Comparison of various lithium silicate sorbents for CO_2 capture performances.

Sorbent	CO_2 Concentration (%) / Temperature (°C)	CO_2 Capture Capacity (g g^{-1})	Kinetics of CO_2 Capture (g g^{-1} min^{-1})	Total Cycles	Last Cycle Capacity (g g^{-1})	Total CO_2 Capture in all cycles (g g^{-1})	References
$LiNO_3$, DFNS	60 /650	0.35	0.22	200	0.35	70.0	This work
Lithium oxalate ($C_2Li_2O_4$), SiO_2 sol	15 /550	0.30	0.01	100	0.27	27.0	Hu et al.[12]
Lithium tartrate ($C_4H_4Li_2O_6$), SiO_2 sol	15 /550	0.27	0.01	50	0.25	12.5	Hu et al.[15]
Lithium acetate dihydrate ($C_2H_3O_2Li{\cdot}2H_2O$), SiO_2 sol	15 /550	0.15	0.05	40	0.25	10.0	Yang et al.[11]
Ethanol solution of $LiNO_3$, diatomite, $NH_3{\cdot}H_2O$	50 /620	0.34	0.16	15	0.33	4.95	Shan et al.[10]
$LiNO_3$, colloidal silica, NH_4OH, microwave processing, $Na_2CO_3/K_2CO_3/Li_2CO_3$ ternary doping	100/700	0.35	0.16	15	0.32	4.80	Subha et al.[5]
$LiOH{\cdot}H_2O$, SiO_2, $C_6H_8O_7$ (chelating agent)	100/680	0.32	0.02	15	0.29	4.35	Wang et al.[7]
LiOH, fumed silica	100/550	0.29	0.26	10	0.29	2.90	Kim et al.[3]
$LiNO_3$, $SiC_8H_{20}O_4$, NH_4F, NH_4OH, C_2H_5OH	100/700	0.26	0.06	10	0.26	2.60	Zubbri et al.[6]
$LiNO_3$, colloidal silica, NH_4OH, microwave processing	100/700	0.32	0.16	10	0.20	2.00	Subha et al.[1]
$LiNO_3$, colloidal silica, NH_4OH	100/700	0.35	0.22	5	0.35	1.75	Subha et al.[1,4]
$LiOH{\cdot}H_2O$, silicon nanopowder or milled silicon	60% /650	0.35	0.22	5	0.25	1.25	Nambo et al.[14]
$LiNO_3$ solution (Li_2CO_3 dissolved in HNO_3 solution), SiO_2 powder	80% /780	0.36	0.19	1	0.36	0.36	Bretado et al.[8]
$LiNO_3$ solution, SiO_2 suspension	80% /650	0.34	0.15	1	0.34	0.34	Ortiz et al.[9]
Li_2CO_3, SiO_2, K_2CO_3 doping	20% /500	0.27	0.07	1	0.27	0.27	Kato et al.[2]
Li_2CO_3, SiO_2	92.5% /600	0.30	0.07	1	0.30	0.30	Izquierdo et al.[4]
$LiNO_3$, silicic acid (H_2SiO_3), glycine	100% /800	0.30	0.02	1	0.30	0.30	Rao et al[13]

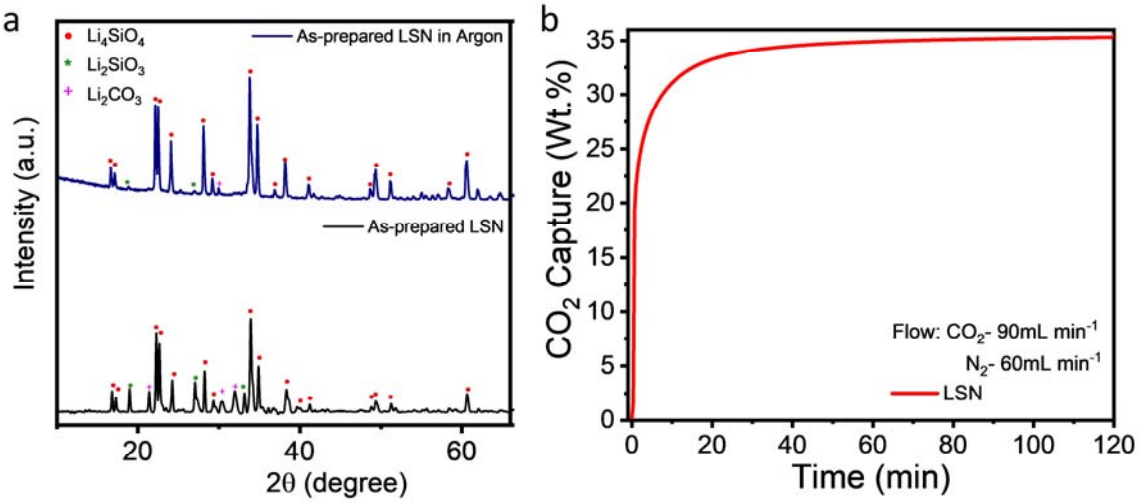

Figure S1. a) PXRD pattern of LSN synthesized under inert atmosphere and b) its CO_2 capture performance.

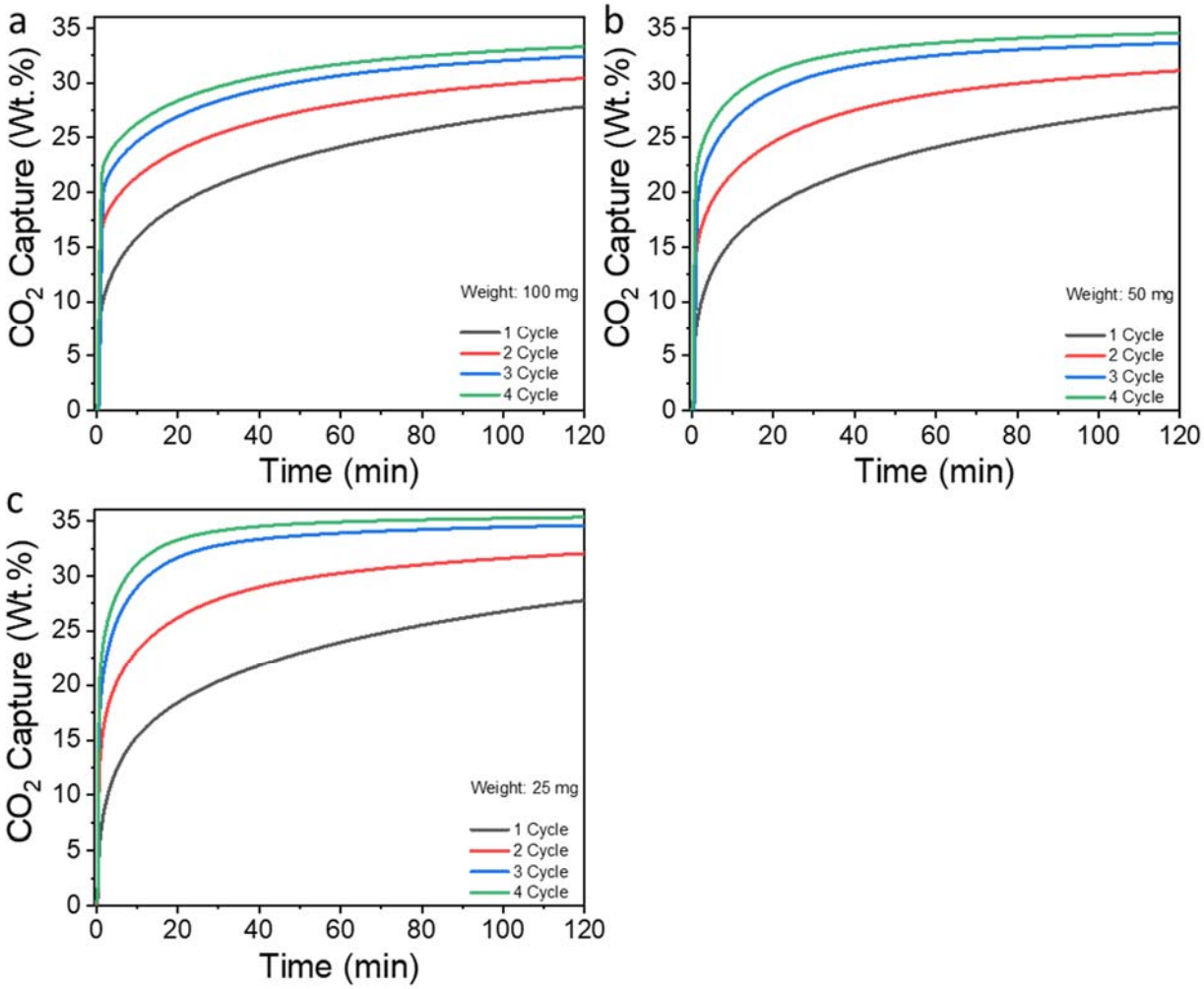

Figure S2. CO_2 capture by LSN using various weights, (a) 100, (b) 50, (c) 25 mg using 60% CO_2 with 150 mL min^{-1} flow at 650 °C.

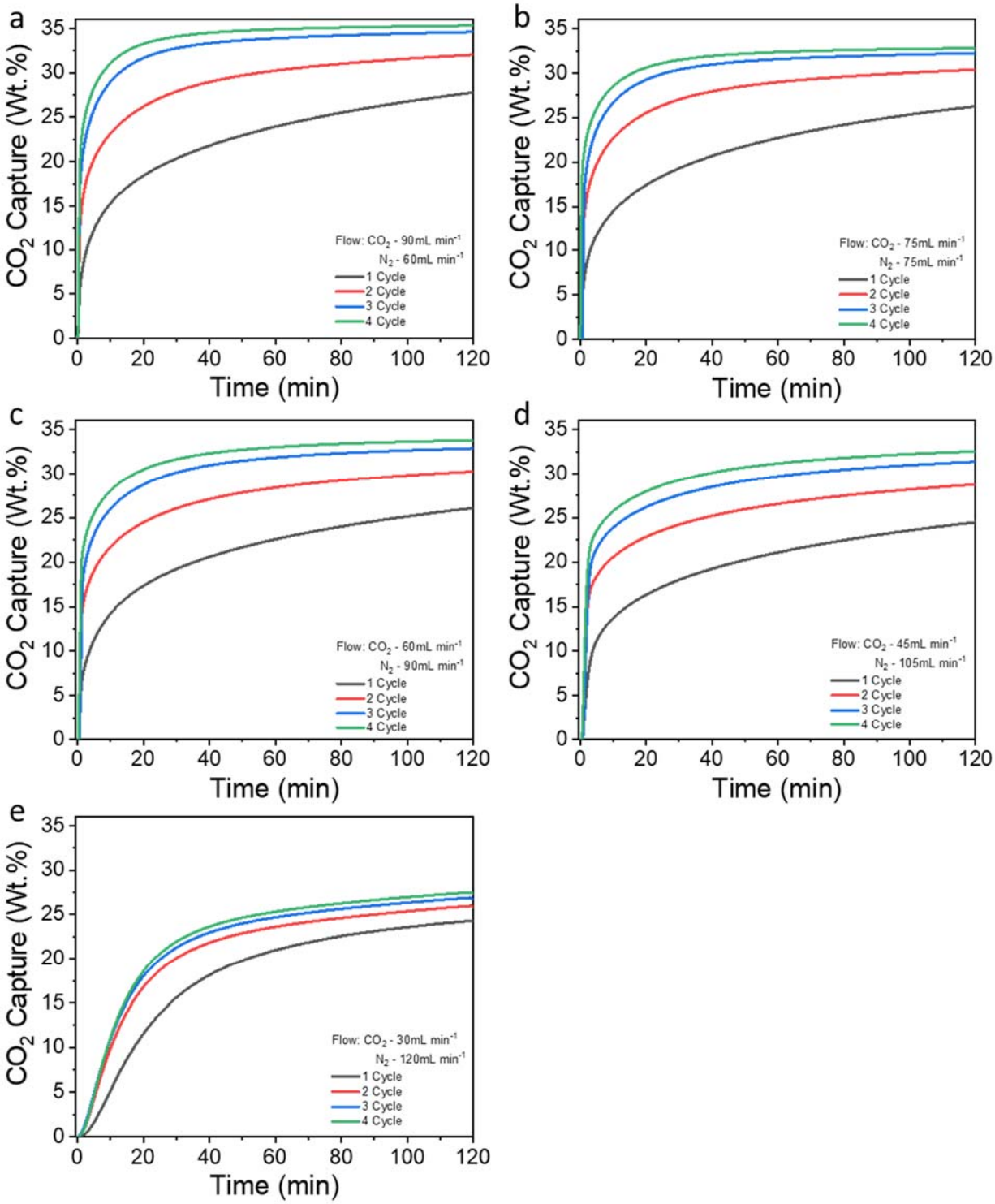

Figure S3. CO_2 capture by LSN at different concentrations of CO_2, (a) 60, (b) 50, (c) 40, (d) 30, (e) 20 % (balanced N_2) using 25 mg of sorbent, 150 mL min^{-1} total flow, at 650 °C.

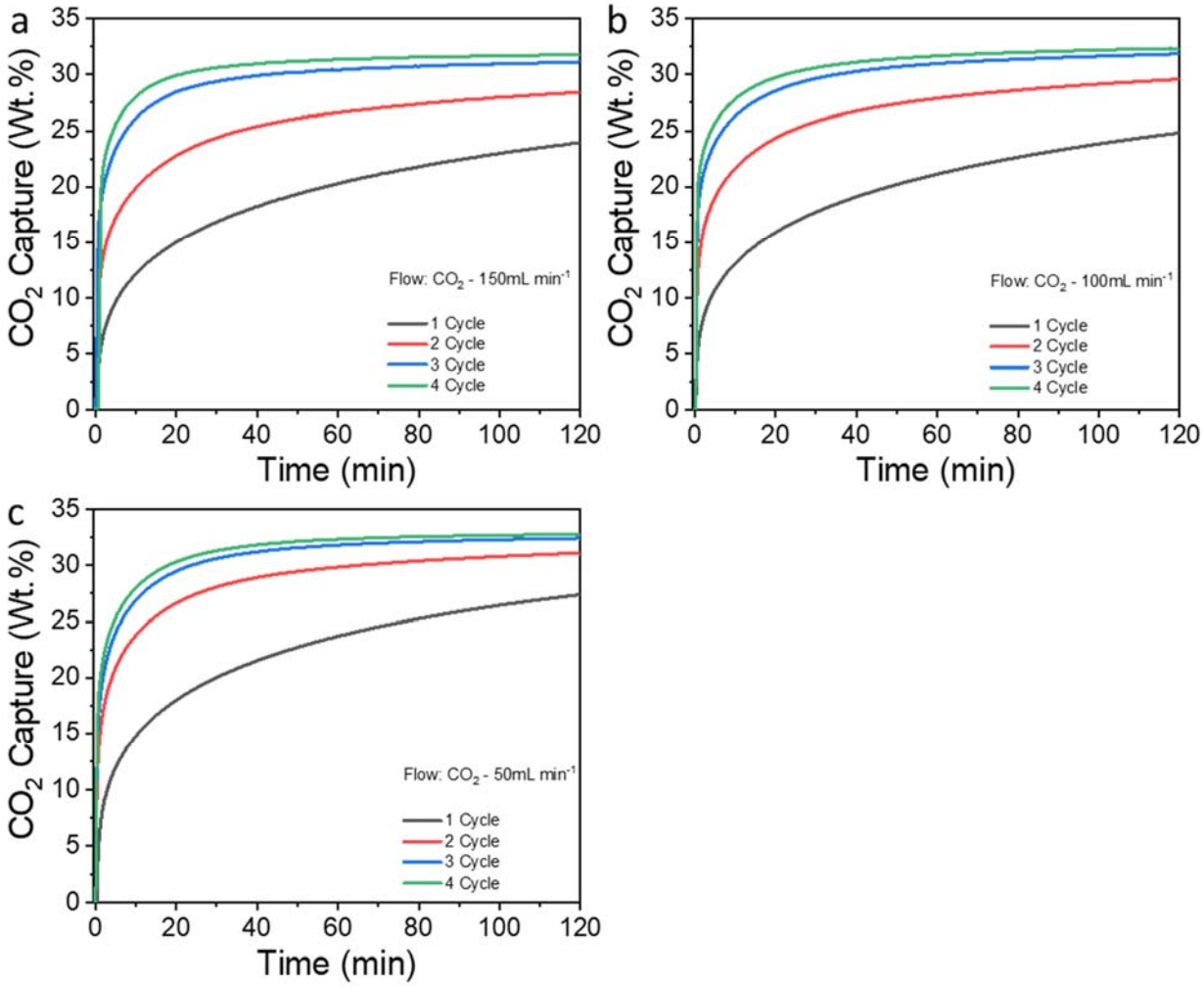

Figure S4. CO_2 capture by LSN at different gas flows, (a) 150, (b) 100, (c) 50 using 25 mg of sorbent with 100% CO_2 at 650 °C.

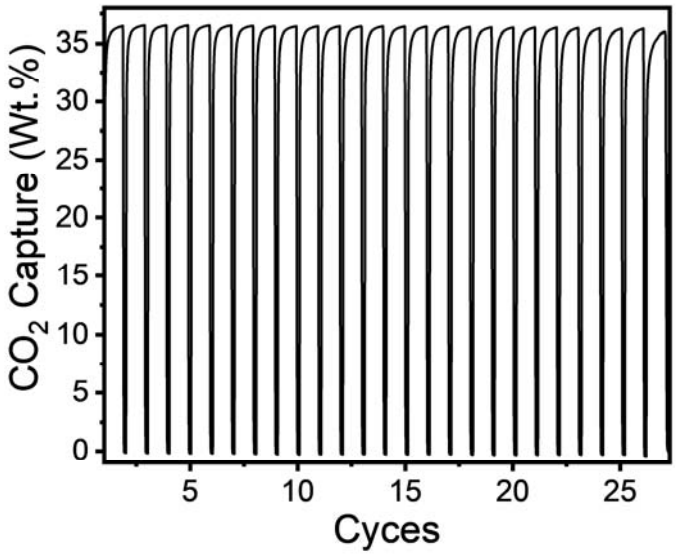

Figure S5. Stability of LSN during CO_2 capture in the presence of water vapors by using 25 mg of sorbent with 60% CO_2 at 650 °C.

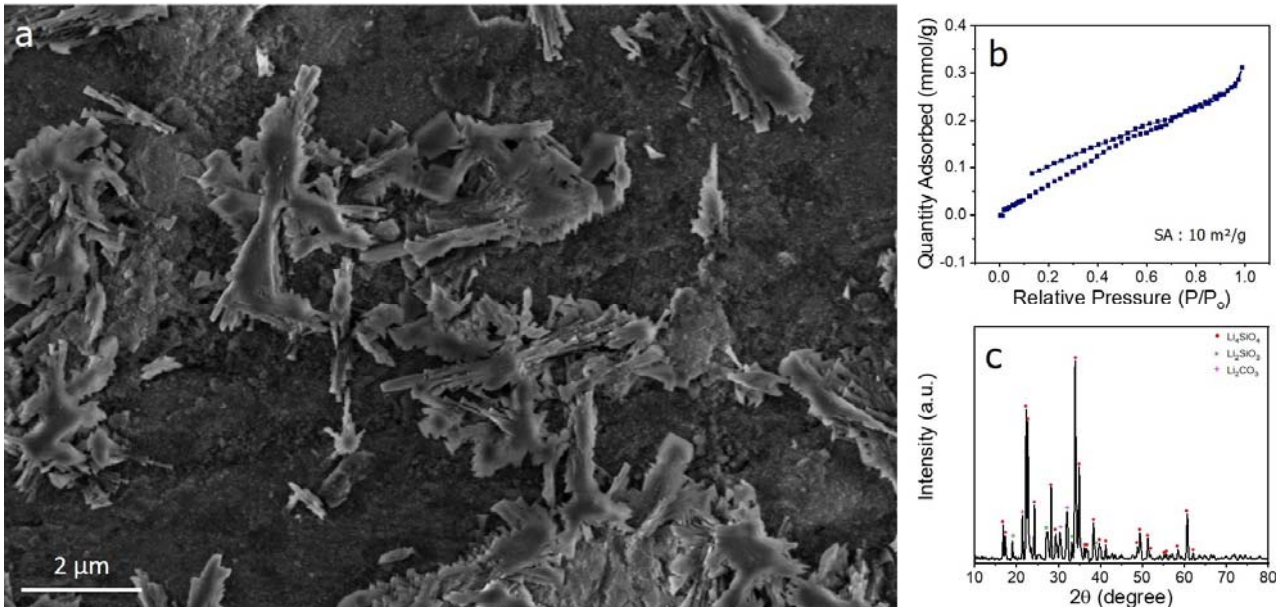

Figure S6. (a) SEM images, (b) N_2 sorption isotherm, and (c) PXRD pattern of LSN after 4-cycles of adsorption-desorption.

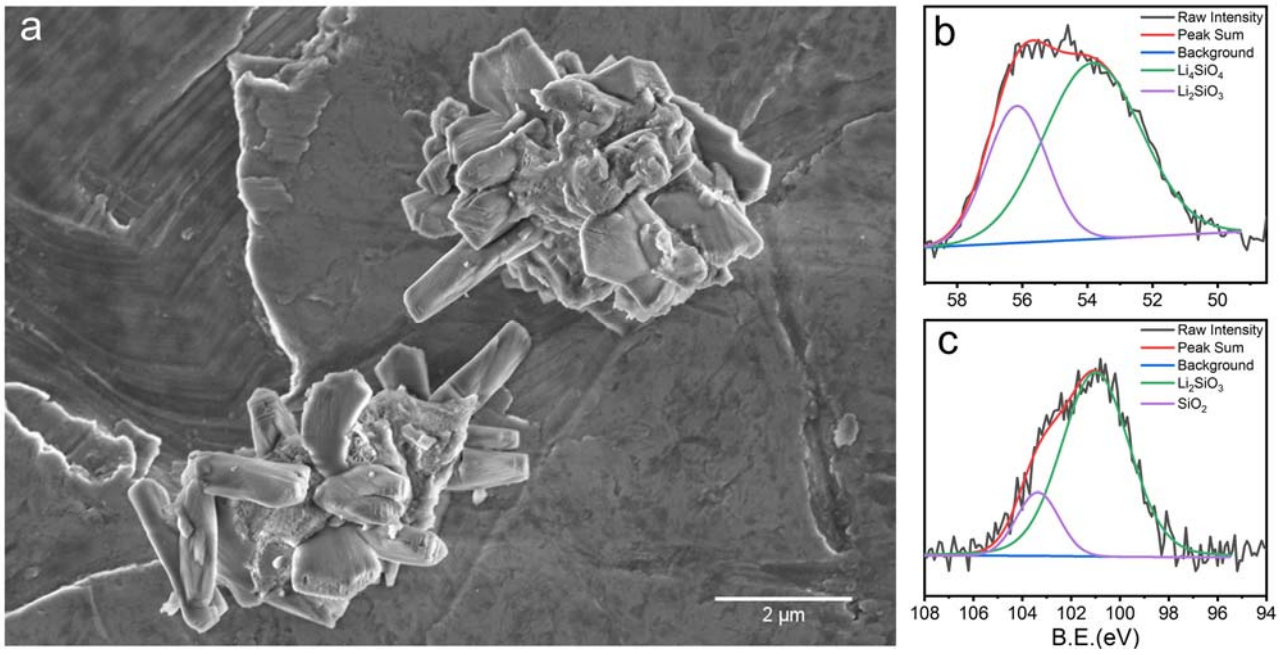

Figure S7. (a) SEM images; XPS spectra of lithium silicates after 200 cycles of CO_2 adsorption-desorption, (b) Li 1s, (c) Si 2p.Binding energy of Li 1s for Li_4SiO_4 and Li_2SiO_3 is ~54 eV and ~55.9 respectivelly.[17-18] The Si $2p_{3/2}$ BE for Li_2SiO_3 is ~102 eV and a very small amount of SiO_2 with B.E of ~104 eV.

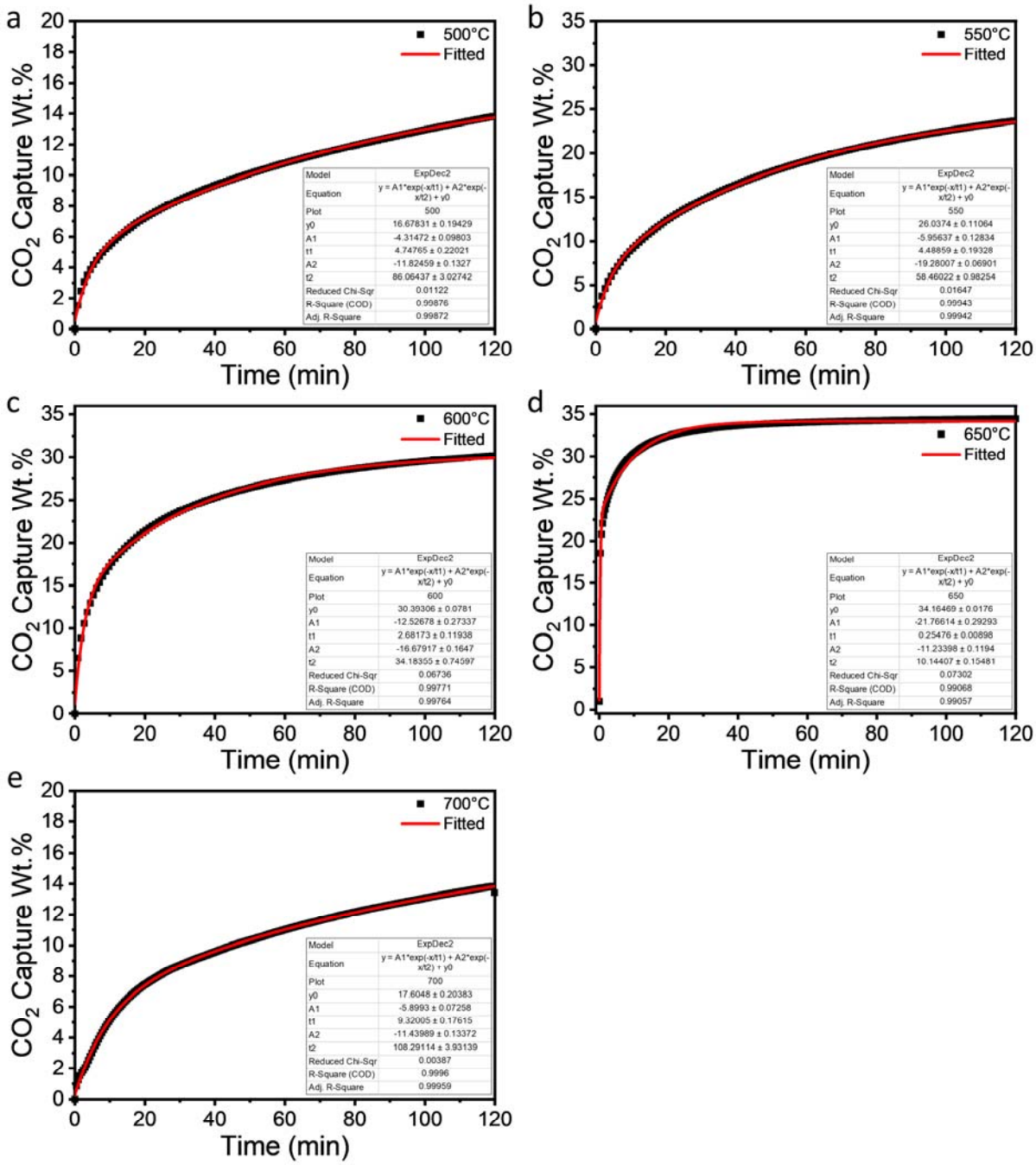

Figure S8. CO_2 capture kinetics of LSN at different temperatures, (a) 500, (b) 550, (d) 600, (d) 650, and (e) 700 °C using 60% CO_2.

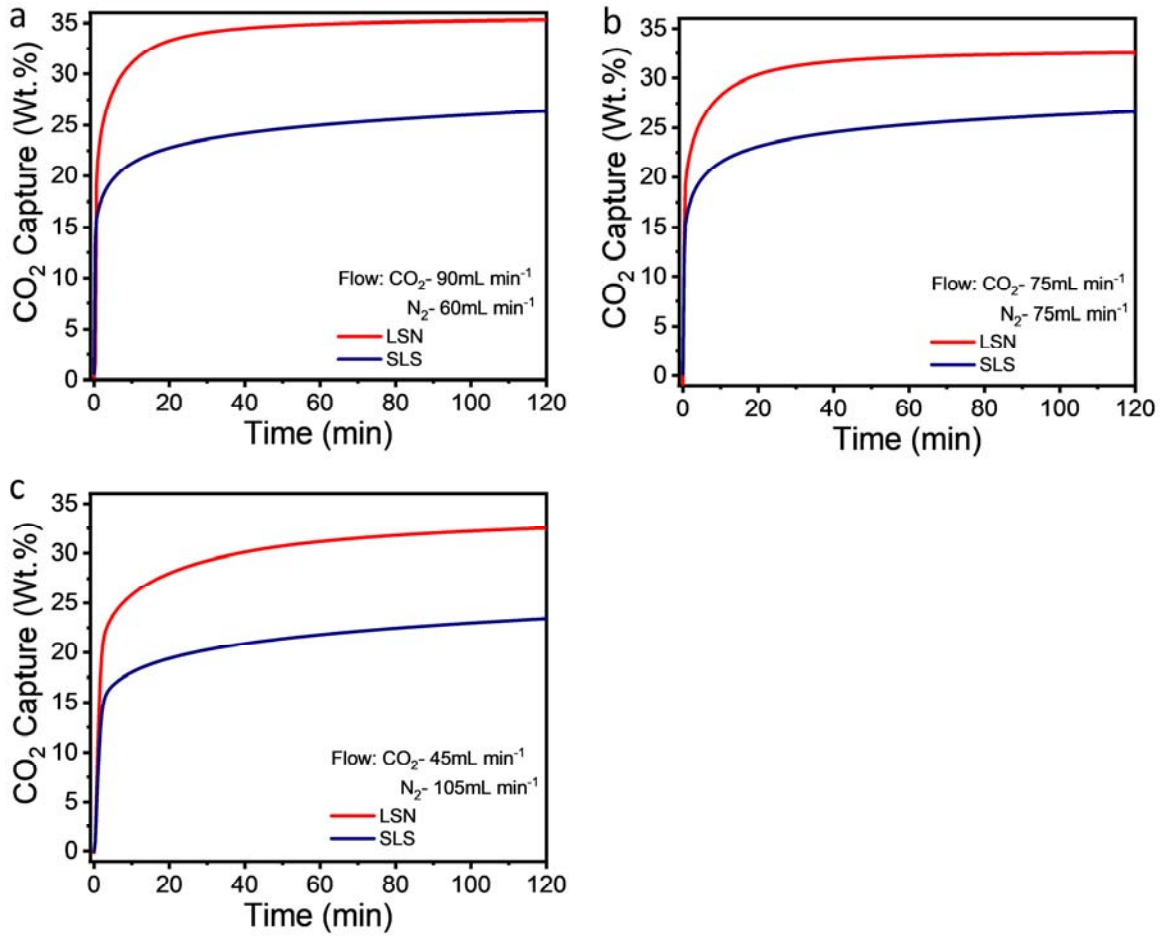

Figure S9. Comparison of LSN and SLS for CO_2 adsorption (rates and capacity) at different concentrations of CO_2, (a) 60, (b) 50, (c) 30 % (balanced N_2) using 25 mg of sorbent, 150 mL min^{-1} total flow, at 650 °C.

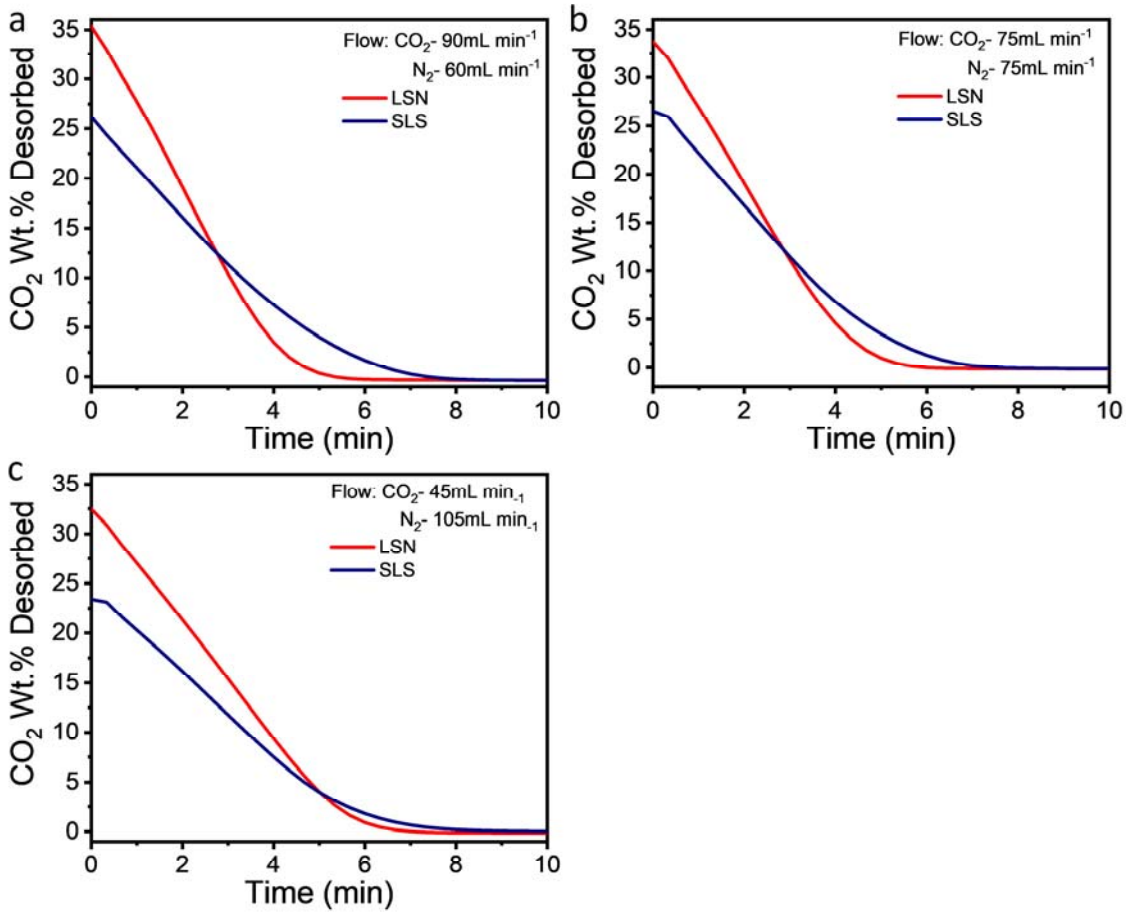

Figure S10. Comparison of LSN and SLS for CO_2 desorption at different concentrations of CO_2, (a) 60, (b) 50, (c) 30 % (balanced N_2) using 25 mg of sorbent, 150 mL min^{-1} total flow, at 650 °C.

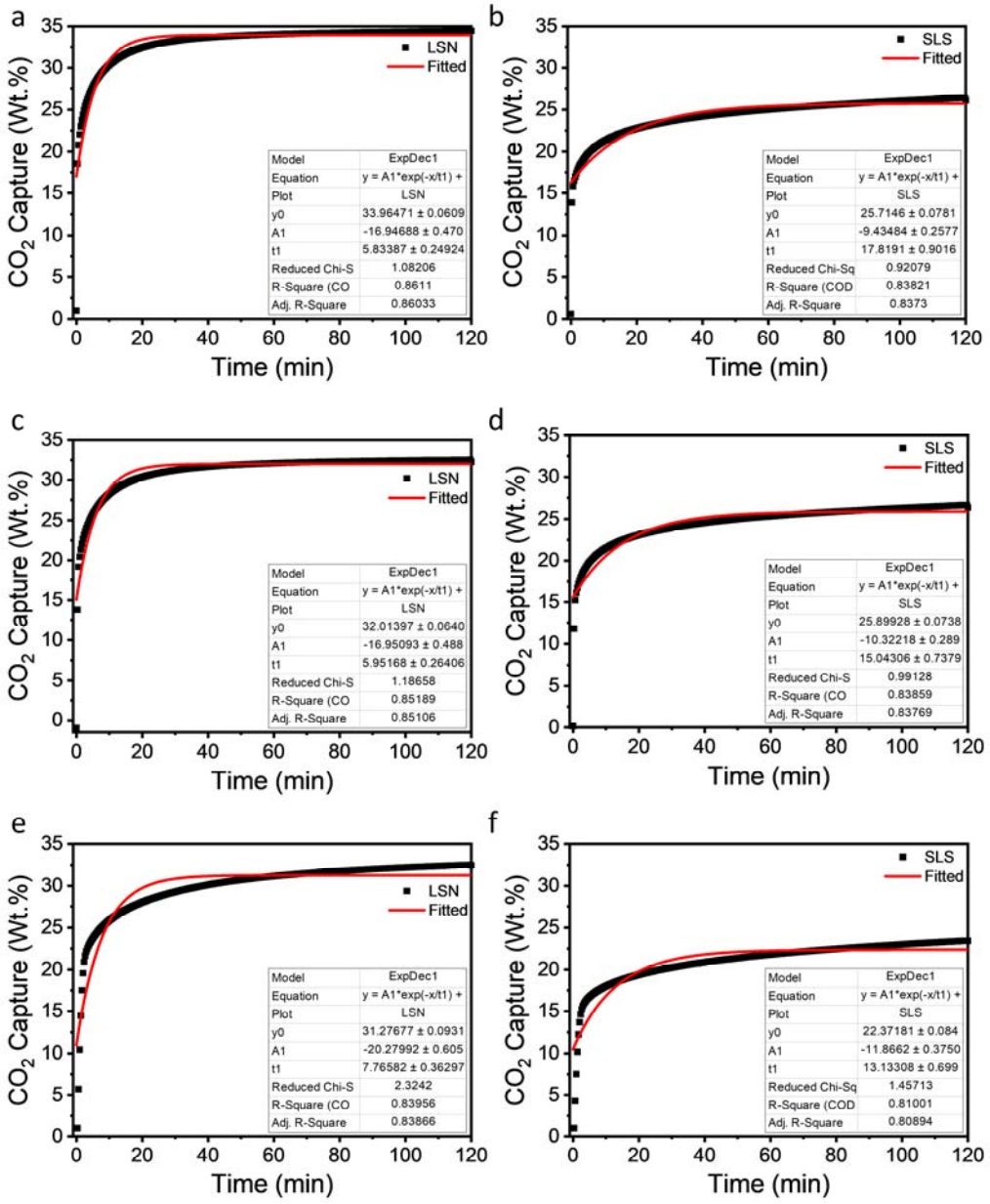

Figure S11. CO_2 capture kinetics fitting in single exponential equation for LSN and SLS at 650°C temperatures using (a) and (b) 60, (c) and (d) 50, (e) and (f) 30 %.

Table S5. Kinetic parameters obtained for LSN and SLS from single exponential adsorption isotherms at 650°C temperatures using different CO_2 flow.

Sample Name	**Gas Flow Percentage (CO_2: N_2)**	**K_1 s^{-1}**	**R^2**
LSN	60:40	0.00285	0.8611
SLS		0.00093	0.8382
LSN	50:50	0.00280	0.8518
SLS		0.00111	0.8385
LSN	30:70	0.00214	0.8395
SLS		0.00127	0.8100

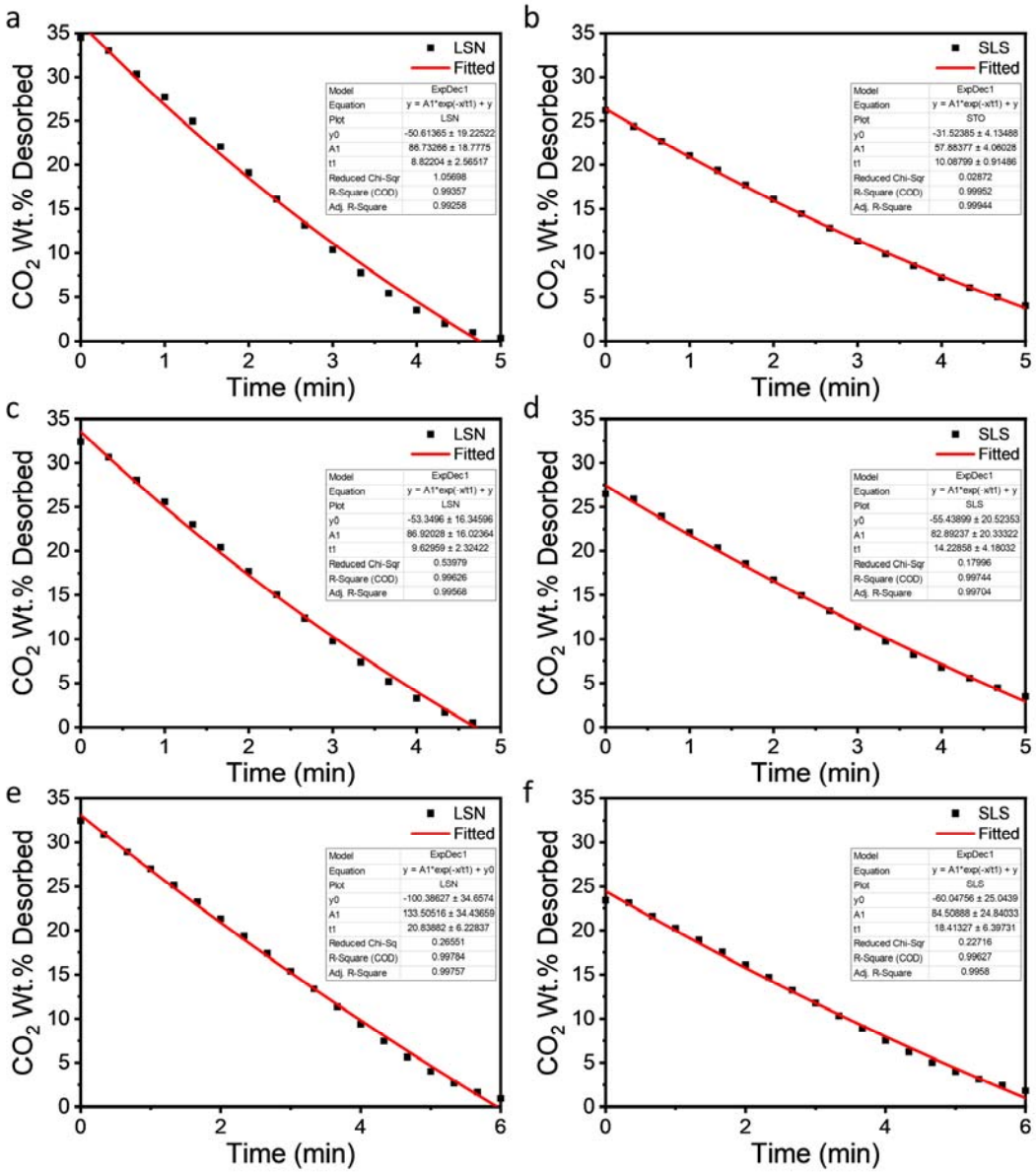

Figure S12. CO_2 desorption kinetics of LSN and SLS fitted in single exponential equation at 650°C temperatures using various CO_2 concentrations, (a) and (b) 60, (c) and (d) 50, (e) and (f) 30 %. $y = A \exp(-k_1 x) + B$ .... Eq. S1, where y-represents the CO_2 adsorbed or desorbed in wt. % respectively, x is the time required to capture CO_2 and desorb CO2, k_1 is the exponential parameters for CO_2 chemisorption and CO2 desorb process, respectively. A is constants, and B is the y-axis intercept.

Table S6. Kinetic parameters obtained from single exponential desorption isotherms fitting at 650°C temperatures.

Sample Name	**Gas Flow Percentage (CO_2:N_2)**	**K_1 s^{-1}**	**R^2**
LSN	60:40	0.002027	0.99357
SLS		0.001652	0.99952
LSN	50:50	0.001731	0.99626
SLS		0.001171	0.99744
LSN	30:70	0.000800	0.99784
SLS		0.000900	0.99627

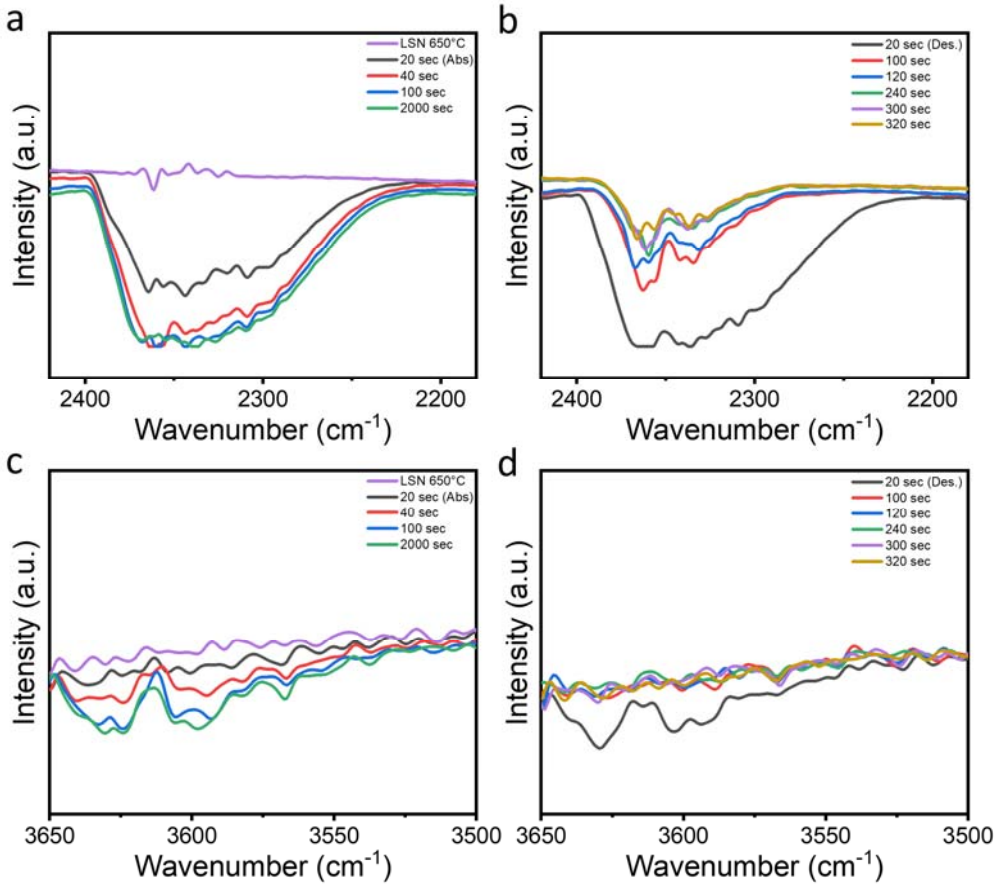

Figure S13. In-situ DRIFT study of CO_2 adsorption-desorption using LSN at 650 °C. FTIR spectra during (a, b) adsorption and (c, d) desorption steps. Adsorption by 60% CO_2 while desorption is by 100% N_2.

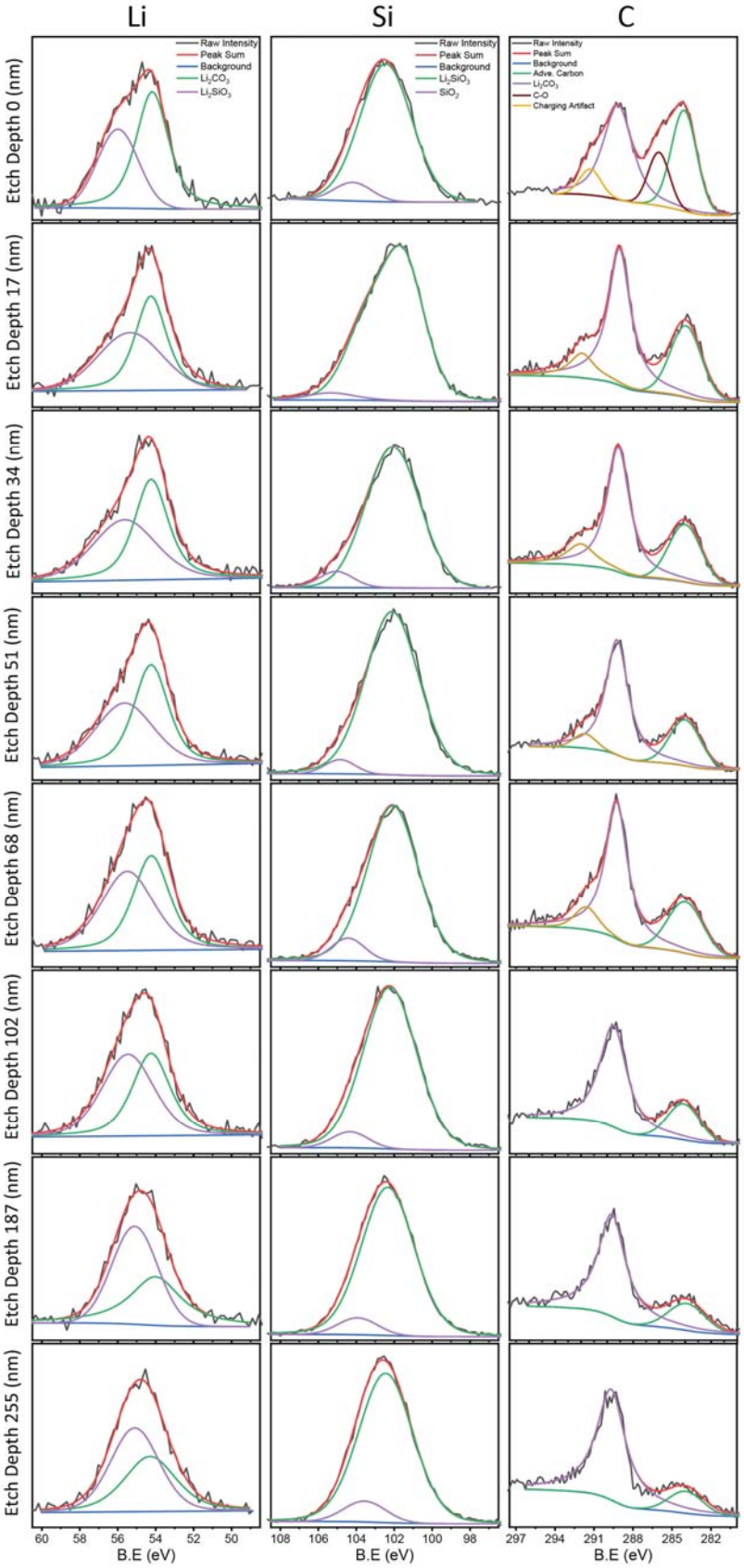

Figure S14. a) XPS fitting of LSN sample with CO_2 kept absorb for Li, Si, C with different etching depth. Binding energy of Li 1s for Li_2CO_3 and Li_2SiO_3 is ~54 eV and ~55.5 respectivelly.[17-18] The Si $2p_{3/2}$ BE for Li_2SiO_3 is ~102 eV and a very small amount of SiO_2 with B.E of ~104 eV. For the C 1s, there are two main peaks corresponding to Li_2CO_3 at ~290 eV and adventitious carbon is at ~284 eV.[17-19] In 0 nm etching, for C 1s XPS, peak at ~286 corresponding to C-O and the peak at ~292 eV due to charging artifact was also observed.[19]

References:

1. P. V. Subha, B. N. Nair, P. Hareesh, A. P. Mohamed, T. Yamaguchi, K. G. K. Warriera and U. S. Hareesh, Enhanced CO_2 absorption kinetics in lithium silicate platelets synthesized by a sol-gel approach, *J. Mater. Chem. A*, 2 (**2014**) 12792-12798.
2. M. Kato, S. Yoshikawa, K. Nakagawa, Carbon dioxide absorption by lithium orthosilicate in a wide range of temperature and carbon dioxide concentrations, *J. Mater. Sci. Lett.* 21 (**2002**) 485–487.
3. H. Kim, H.D. Jang, M. Choi, Facile synthesis of macroporous Li_4SiO_4 with remarkably enhanced CO_2 adsorption kinetics, *Chem. Eng. J.* 280 (**2015**) 132–137.
4. M.T. Izquierdo, A. Turan, S. Garcia, M.M. Maroto-Valer, Optimization of Li_4SiO_4 synthesis conditions by a solid state method for maximum CO_2 capture at high temperature, *J. Mater. Chem. A* 6 (**2018**) 3249–3257.
5. P.V. Subha, B.N. Nair, A.P. Mohamed, G.M. Anilkumar, K.G.K. Warrier, T. Yamaguchi, U.S. Hareesh, Morphologically and compositionally tuned lithium silicate nanorods as high-performance carbon dioxide sorbents, *J. Mater. Chem. A* 4 (**2016**) 16928–16935.
6. N.A. Zubbri, A.R. Mohamed, M. Mohammadi, Parametric study and effect of calcination and carbonation conditions on the CO_2 capture performance of lithium orthosilicate sorbent, *Chin. J. Chem. Eng.* 26 (**2018**) 631–641.
7. K. Wang, X. Wang, P. Zhao, X. Guo, High-temperature capture of CO_2 on lithiumbased sorbents prepared by a water-based sol-gel technique, *Chem. Eng. Technol.* 37 (**2014**) 1552–1558.
8. M.E. Bretado, V. Guzman Velderrain, D. Lardizabal Gutierrez, V. Collins-Martinez, A.L. Ortiz, A new synthesis route to Li_4SiO_4 as CO_2 catalytic/sorbent, *Catal. Today* 107–108 (**2005**) 863–867.
9. Lopez Ortiz, M.A. Escobedo Bretado, V. Guzman Velderrain, M. Melendez Zaragoza, J. Salinas Gutierrez, D. Lardizabal Gutierrez, V. Collins-Martinez, Experimental and modeling kinetic study of the CO_2 absorption by Li_4SiO_4, *Int. J. Hydro. Eng.* 39 (**2014**) 16656–16666.
10. S. Shan, S. Li, Q. Jia, L. Jiang, Y. Wang, J. Peng, Impregnation precipitation preparation and kinetic analysis of Li_4SiO_4-based sorbents with fast CO_2 adsorption rate, *Ind. Eng. Chem. Res.* 52 (**2013**) 6941–6945.
11. X. Yang, W. Liu, J. Sun, Y. Hu, W. Wang, H. Chen, Y. Zhang, X. Li, M. Xu, Preparation of novel Li_4SiO_4 sorbents with superior performance at low CO_2 concentration, *ChemSusChem* 9 (**2016**) 1607–1613.
12. Y. Hu, W. Liu, Y. Yang, X. Tong, Q. Chen, Z. Zhou, Synthesis of highly efficient, structurally improved Li_4SiO_4 sorbents for high-temperature CO_2 capture, *Ceram Int.* 44 (**2018**) 16668–16677.
13. G.J. Rao, R. Mazumder, S. Bhattacharyya, P. Chaudhuri, Synthesis, CO_2 absorption property and densification of Li_4SiO_4 powder by glycine-nitrate solution combustion method and its comparison with solid state method, *J. Alloys Compd.* 725 (**2017**) 461–471.
14. Nambo, J. He, T.Q. Nguyen, V. Atla, T. Druffel, M. Sunkara, Ultrafast carbon dioxide sorption kinetics using lithium silicate nanowires, *Nano Lett.* 17 (**2017**) 3327–3333.
15. Y. Hu, W. Liu, Z. Zhou, Y. Yang, Preparation of Li_4SiO_4 sorbents for carbon dioxide capture via a spray-drying technique, *Eng. Fuel* 32 (**2018**) 4521–4527.
16. P. V. Korake, A. G. Gaikwad *Front. Chem. Sci. Eng.* 5 (**2011)** 215–226.
17. J. F. Moulder, W. F. Stickle, P E.'Sobol, K D. Bomben, Eds. J. Chastain, *Perkin-Elmer Corporation Physical Electronics Division*, (**1992)** 34–35.
18. Kevin N. Wood and Glenn Teeter, *ACS Appl. Energy Mater.* 1 (**2018)** 4493–4504.